Robust Adaptive Consensus Control of Fractional-Order Multi-Agent Systems Using BBO-Optimized Type-2 Fuzzy Neural Networks

Ping Yu[1], Hafiza Tabinda Rauf[2,*], Meraa Arab[3,*] and Salma Trabelsi[3]

[1] Hefei Technology College, Hefei, China

[2] Department of Mathematics and Statistics, The University of Lahore, Sargodha, Pakistan

[3] Department of Mathematics and Statistics, College of Science, King Faisal University, Al Ahsa, Saudi Arabia

INFORMATION

Keywords:
Fractional-order multi-agent systems
adaptive control
RGT2FNN
BBO optimization
input saturation
time-varying delays

DOI: 10.23967/j.rimni.2026.10.78686

SCIPEDIA Revista Internacional de Métodos Numéricos para Cálculo y Diseño en Ingeniería

Revista Internacional Métodos numéricos para cálculo y diseño en ingeniería RIMNI

In cooperation with CIMNE

Robust Adaptive Consensus Control of Fractional-Order Multi-Agent Systems Using BBO-Optimized Type-2 Fuzzy Neural Networks

Ping Yu[1], **Hafiza Tabinda Rauf**[2,*], **Meraa Arab**[3,*] **and Salma Trabelsi**[3]

[1]Hefei Technology College, Hefei, China

[2]Department of Mathematics and Statistics, The University of Lahore, Sargodha, Pakistan

[3]Department of Mathematics and Statistics, College of Science, King Faisal University, Al Ahsa, Saudi Arabia

ABSTRACT

The consensus control problem to be discussed in this paper is concerned with nonlinear multi-agent systems with unknown dynamics, unknown fractions, time-varying delays, and input saturation limits. In order to address these difficulties, an adaptive control system is established, incorporating a recurrent general type-2 fuzzy neural network (RGT2FNN) with a biogeography-based optimization (BBO) algorithm. The RGT2FNN is used to model nonlinear functions that are not known offline, and the BBO algorithm also optimizes the parameters of the fuzzy network and performs offline identification of the fractional order by minimizing multi-step model prediction error. In order to make the model more resistant to modeling uncertainties, time-varying delays, and actuator saturation effects, a LMI-based compensator is proposed to ensure the stability of the closed-loop. Lyapunov analysis guarantees the boundedness of consensus errors. The simulation findings prove that the suggested methodology can attain an accurate consensus tracking and strong performance when the uncertainties are harsh, the delays may change with time, and the limits of input saturation are taken into account.

OPEN ACCESS

Received: 06/01/2026

Accepted: 16/03/2026

DOI
10.23967/j.rimni.2026.10.78686

Keywords:
Fractional-order multi-agent systems
adaptive control
RGT2FNN
BBO optimization
input saturation
time-varying delays

1 Introduction

The study of consensus in fractional-order multi-agent systems (MAS) has attracted significant attention due to their ability to capture long-term memory and hereditary effects in dynamical networks [1,2]. Unlike integer-order systems, fractional-order MAS naturally model non-local dynamics, which is crucial for applications requiring history-dependent behavior [3,4]. These systems are particularly relevant in robotics, cooperative vehicle networks, and energy systems, where the agents' interactions and past states influence future evolution [5].

Achieving consensus in fractional-order MAS is challenging, especially when the fractional orders are unknown. Unknown-order identification adds modeling uncertainty, complicating control design and stability analysis [6,7].

*Correspondence: Hafiza Tabinda Rauf, Meraa Arab (tabindarauf2000@gmail.com, marab@kfu.edu.sa).

Time-varying communication delays are another major challenge in practical MAS implementations [8,9]. Delays introduce outdated information into the feedback loop, which may degrade damping and induce oscillations. In fractional-order systems, such delays are further amplified due to the memory property of fractional derivatives, which accumulate historical states over time [10,11]. Consequently, delay-dependent stability analysis is necessary to guarantee safe operation in real-world scenarios. Actuator input saturation is a common physical limitation that can prevent MAS from achieving ideal performance [12]. To address uncertainties, nonlinearities, and unknown dynamics, fuzzy logic and neural network-based approximators have been widely adopted [13–17]. These methods allow the MAS to adaptively learn system behavior, compensate for unknown parameters, and maintain desired performance. Event-triggered neural learning and distributed Q-learning frameworks have further enhanced adaptability by reducing communication burden while ensuring convergence.

Robust formation control of MAS in dynamic environments also relies on prescribed performance metrics and observer-based strategies [18–20]. Sliding mode control, fixed-time disturbance rejection, and anti-unwinding attitude tracking provide guaranteed performance in the presence of uncertainties, delays, and nonlinear couplings [21,22]. Such strategies have been applied in aerial swarms, robotic manipulators, and space systems, demonstrating their versatility.

Hierarchical and hybrid control approaches have also been proposed to manage high-dimensional systems and multi-layer interactions [23–27]. Similarly, hybrid nominal-robust designs ensure hub motors [28–32], microgrids, and pneumatic systems operate reliably under both parametric and nonparametric uncertainties [33–37].

The following research questions provide a motivation to conduct this study:

- **RQ1:** How can a robust control protocol be developed with multi-agent systems when the nonlinear dynamics and the fractional orders (q) are entirely unknown?
- **RQ2:** Does a recurrent structure incorporated in a General Type-2 Fuzzy Neural Network effectively capture temporal dependencies and high level uncertainties of a fractional-order dynamics?

2 Preliminaries

Graph Theory

The communication topology among the N follower agents and the leader is modeled by a directed graph $\mathcal{G} = (\mathcal{V}, \mathcal{E}, \mathcal{A})$, where $\mathcal{V} = \{1, 2, \ldots, N\}$ is the set of nodes, $\mathcal{E} \subseteq \mathcal{V} \times \mathcal{V}$ denotes the edge set, and $\mathcal{A} = [a_{ij}] \in \mathbb{R}^{N\times N}$ is the weighted adjacency matrix with $a_{ij} > 0$ if $(j, i) \in \mathcal{E}$ and $a_{ij} = 0$ otherwise. The Laplacian matrix is defined as $L = D - \mathcal{A}$, where D is the in-degree matrix.

Assumption 1: *The directed communication graph contains a spanning tree rooted at the leader, and at least one follower is pinned to the leader, i.e., $\exists i$ such that $b_i > 0$.*

Assumption 2: *The unknown nonlinear functions $f_i(\cdot)$ and disturbances $d_i(t)$ are continuous and bounded,*

$$\|f_i(x)\| \le \bar{f}_i, \quad \|d_i(t)\| \le \bar{d}_i.$$

Assumption 3: *The time-varying delays $\tau_i(t)$ satisfy $0 \le \tau_i(t) \le \bar{\tau}$, where $\bar{\tau}$ is a known constant. Furthermore, the rate of variation of the time-varying delay $\tau_i(t)$ is assumed to be bounded such that: $\dot{\tau}_i(t) \le \mu < 1$ where μ is a known constant.*

Assumption 4: *The fractional order satisfies $0 < q < 1$, and its estimate $\hat{q}$ remains bounded.*

Lemma 1: *[18] Let $x(t) \in \mathbb{R}^n$ be a continuously differentiable vector function. Then, for any time instant $t \geq t_0$, the following inequality holds for the Caputo fractional derivative of order $q \in (0,1)$:*

$$\frac{1}{2} D_t^q \left(x^T(t) x(t) \right) \leq x^T(t) D_t^q x(t), \quad \forall t \geq t_0$$

3 Problem Formulation

A category of FOMASs is examined, where the dynamics of the ith agent are represented as:

$$D_t^q x_i^1(t) = x_i^2(t), \quad D_t^q x_i^2(t) = x_i^3(t), \ldots, \quad D_t^q x_i^n(t) = f_i(x_i(t - \tau_i(t))) + \text{sat}(u_i(t)) + d_i(t) \tag{1}$$

where $x_i = [x_i^1, \ldots, x_i^n]^T \in \mathbb{R}^n$, $f_i(x_i(t - \tau_i(t)))$ is an unknown but bounded function, $\tau_i(t)$ denotes an unknown time-varying delay, d_i is a disturbance, $sat(u_i(t)) \in \mathbb{R}$ is the saturation control input for follower i, and q corresponds to the fractional-order value in the sense of the Caputo definition. The actuator saturation nonlinearity is defined as

$$\text{sat}(u_i) = \begin{cases} u_{i,\min}, & u_i < u_{i,\min}, \\ u_i, & u_{i,\min} \leq u_i \leq u_{i,\max}, \\ u_{i,\max}, & u_i > u_{i,\max}, \end{cases} \tag{2}$$

where $u_{i,\min}$ and $u_{i,\max}$ denote the known lower and upper bounds of the actuator input. The leader agent dynamic is provided as follows:

$$D_t^q x_0^1 = x_0^2, \quad D_t^q x_0^2 = x_0^3, \ldots, \quad D_t^q x_0^n = f_0(x_0(t - \tau(t))) \tag{3}$$

where, $x_0 = [x_0^1, \ldots, x_0^n]^T \in \mathbb{R}^n$. The proposed fuzzy systems approximate the dynamics of each agent offline as follows:

$$D_t^{\hat{q}} \hat{x}_i^1 = \hat{x}_i^2, \quad D_t^{\hat{q}} \hat{x}_i^2 = \hat{x}_i^3, \ldots, \quad D_t^{\hat{q}} \hat{x}_i^n = \hat{f}_i \hat{x}_i + \text{sat}(u_i) \tag{4}$$

where $\hat{q}$ and $\hat{f}_i$ represent the estimates of q and $f_i + d_i$, respectively. $\hat{x}_1^i, \ldots, \hat{x}_i^n$ are the estimations of $x_1^i, \ldots, x_i^n$, respectively. Fig. 1 illustrates the proposed control scheme.

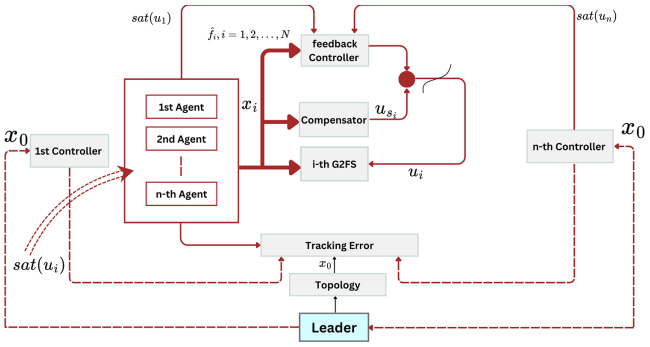

Figure 1: Block diagram of the proposed control framework. The leader and follower states are processed through the RGT2FNN-based adaptive controller.

Control Objective

The objective of this paper is to design a distributed adaptive control protocol for nonlinear fractional-order multi-agent systems such that all followers asymptotically track the leader. Specifically, under Assumptions 1–4, the control objective is to guarantee leader-following consensus in the

sense that

$$\lim_{t\to\infty} \|x_i(t) - x_0(t)\| = 0, \quad \forall i = 1, \ldots, N,$$

or equivalently, $\lim_{t\to\infty} \|e_i(t)\| = 0$, where $e_i(t)$ denotes the local neighborhood tracking error defined in (10). Furthermore, all closed-loop signals are required to remain bounded.

4 Recurrent General Type-2 Fuzzy Neural Network Model

The RGT2FNN is introduced to estimate nonlinear functions with time-varying delays. As shown in Fig. 2, this model extends conventional type-2 fuzzy systems. The general type-2 fuzzy set $\tilde{\varrho}$ is formulated as follows [17]:

$$\tilde{\varrho} = \int_{x\in X} \int_{u\in[0,1]} \mu_{\tilde{\varrho}}(x,u)/(x,u)$$

where x and u denote the primary and secondary variables. Additionally, $\mu_{\tilde{\varrho}}(x,u)$ represents the type-2 MF.

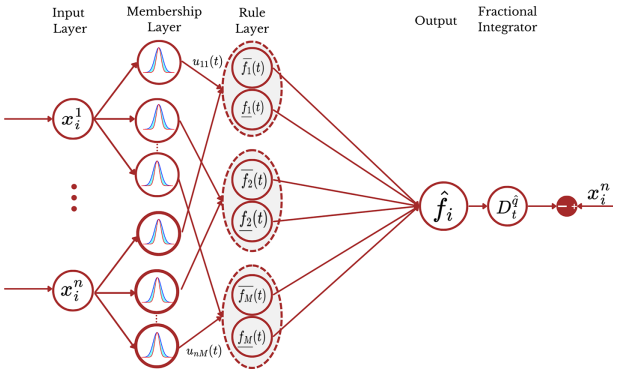

Figure 2: Structure of RGT2FNN. The inputs are the agent states, which pass through upper and lower membership functions.

To approximate unknown functions, the state variables, denoted as $x_i = [x_1^i, \ldots, x_i^k, \ldots, x_i^n]^T$, where $k = 1, \ldots, n$, are used as inputs. The jth membership function for the kth input, represented as $\tilde{\varrho}_k^j$, is assumed to have a footprint of uncertainty modeled by a Gaussian function. The RGT2FNN generates an output as:

Step 1: The upper and lower membership functions of $\tilde{\varrho}_k^j$ are computed as:

$$\bar{\mu}_{jk}(t) = \exp\left(-\left[\frac{x_i^k(t) + \kappa\bar{\mu}_{jk}(t-1) - c_{jk}}{\bar{\sigma}_{jk}}\right]^2\right), \quad \underline{\mu}_{jk}(t) = \exp\left(-\left[\frac{x_i^k(t) + \kappa\underline{\mu}_{jk}(t-1) - c_{jk}}{\underline{\sigma}_{jk}}\right]^2\right)$$

where $i = 1, \ldots, N$ is the agent index; $k = 1, \ldots, n$ is the input index; and $j = 1, \ldots, M$ is the rule index. $\bar{\mu}_{jk}(t)$ and $\underline{\mu}_{jk}(t)$ represent the upper and lower membership grades, respectively. $\kappa \in [0,1]$ is the recurrence gain (temporal smoothing factor), c_{jk} denotes the center of the j-th membership function for the k-th input and $\bar{\sigma}_{jk}$ and $\underline{\sigma}_{jk}$ represent the upper and lower widths (spreads) of the Gaussian function, respectively, defining the footprint of uncertainty (FOU) [18].

Step 2: Each rule is structured as follows:

Rule^{l}: if x_1^i is $\tilde{\varrho}_1^l$ and $\cdots$ and x_i^k is $\tilde{\varrho}_k^l$ and $\cdots$ and x_i^n is $\tilde{\varrho}_n^l$ then φ is $\tilde{M}^{*l}$, $l = 1, \ldots, M$

where $\tilde{M}^{*l}$ represents the lth membership function, and φ denotes the output of the RGT2FNN. Additionally, M indicates the total number of rules.

Step 3: Each rule's firing strength and consequent parameter are denoted by z_l and w_l, respectively. The Nie-Tan type-reduction method is utilized to get the output as: $\varphi = \dfrac{\sum_{v=1}^{N_\beta} \beta_v W^T \vartheta}{\sum_{v=1}^{N_\beta} \beta_v}$ where, $\vartheta = [z_1, \ldots, z_M]^T$, $W = [w_1, \ldots, w_M]^T$, $z_l = ((\overline{z}_l + \underline{z}_l)/2)/\sum_{l=1}^{M}((\overline{z}_l + \underline{z}_l)/2)$. Here β_v denotes the v-th β-cut, where $v = 1, \ldots, N_\beta$ and N_β is the number of β-cuts. Here, $\beta \in [0, 1]$ represents the β-cut level for the secondary membership function, and N_β denotes the total number of discretization levels for the type-reduction process.

For the l-th fuzzy rule, the upper and lower firing strengths are defined as $\overline{z}_l(t) = \prod_{k=1}^{n} \overline{\mu}_{lk}(t)$, $\underline{z}_l(t) = \prod_{k=1}^{n} \underline{\mu}_{lk}^{L}(t)$, where $\overline{\mu}$ and $\underline{\mu}$ denote the upper and lower membership grades of the k-th input in the l-th rule.

5 Optimization Using BBO Algorithm

The optimization process is explained in detail below.

1. Population initialization occurs first in the process where each individual serves as a solution potential to determine the parameters. The specific parameters are outlined as: $\theta_i = [w_1^i, \ldots, w_M^i, \hat{q}_i]^T$. The parameters $w_1^i, \ldots, w_M^i$ describe the h-th RGT2FNN while the estimated fractional-order is referred to as $\hat{q}_i$. The first population section P_i contains n_p individual members. During the optimization, the search space for $\hat{q}$ is constrained to $\hat{q} \in [0.01, 0.99]$ to satisfy Assumption 4.
2. Formulate the immigration and emigration rate definitions using these terms: $\lambda_h = (h-1)/n_p$, $\gamma_h = 1 - (h-1)/n_p$, $h = 1, \ldots, n_p$ where, immigration rates marked as λ_h together with emigration rates indicated as γ_h.
3. Determine the evaluation of each individual through the given cost function: $J_h = \sum_{k=1}^{T} \left\| x_i(t_k) - \hat{x}_i(t_k; \theta_h) \right\|^2$, where $\hat{x}_i(t_k; \theta_h)$ is the predicted state trajectory generated using the candidate fractional order $\hat{q}_h$ and RGT2FNN parameters w_h over sampling horizon T.
4. The identification process is performed over a dataset of N_s trajectories generated via preliminary system excitation. We set the sampling period $h = 0.01$ s and a prediction horizon $T = 50$ steps.
5. Generate a random number n_h within the interval $[0, 1]$ for each individual. If $n_h \leq \lambda_h$, then randomly choose the individual P_h' and update P_h using the following rule:

$$P_h(t+1) = P_h(t) + \varsigma \left(P_h'(t) - P_h(t) \right)$$

Here, $0 < \varsigma \leq 1$ denotes the adaptation rate.

6. Assess the newly generated individuals P_h' for $h = 1, \ldots, n_p$ and choose n_p from the combined set of newly generated individuals P_h', where $h = 1, \ldots, n_p$, and existing individuals P_h.

With a population size $n_p = 40$ and 100 generations, the offline optimization requires 4000 objective function evaluations.

Lemma 2 ([19]): *If the dynamics of both the plant and the controller are given by:*

$$\begin{cases} P: & D^q x = Ax + B_1 \mathrm{sat}(u) + B_2 \omega,\ y = C_1 x + D_1 \mathrm{sat}(u) + D_2 \varpi,\ z = C_2 x + D_3 \mathrm{sat}(u) + D_4 \varpi; \\ K: & D^q x_c = A_c x_c + B_c y,\ u = C_c x_c + D_c y \end{cases} \tag{5}$$

Then stability of system is ensured if we have matrices $X = X^T \in \mathbb{R}^{2n\times 2n}$, $Z = Z^T \in \mathbb{R}^{n\times n}$, and $H = H^T \in \mathbb{R}^{n\times n}$ subject to the satisfaction of the following LMIs:

$$\begin{bmatrix} \bar{r}(AZ + B_1\hat{C}) + r(ZA^T + \hat{C}^T B_1^T) & \bar{r}(HA + \hat{B}C_1) + r(A^T H + C_1^T \hat{B}^T) & B_2 + B\hat{D}D_2 & \bar{r}(C_2 Z + D_3\hat{C})^T \\ r(A + B_1\hat{D}C_1)^T + \bar{r}\hat{A} & (HB_2 + \hat{B}D_4)^T & HB_2 + \hat{B}D_2 & -\bar{r}(C_2 + D_3\hat{D}C)^T \\ (B_2 + B_1\hat{D}D_4)^T & r(C_2 + D_3\hat{D}C_1) & -\gamma^2 I & (D_4 + D_3\hat{D}D_2)^T \\ r(C_2 Z + D_3\hat{C}) & \bar{r}(HA + \hat{B}C_1) + r(A^T H + C_1^T \hat{B}^T) & D_4 + D_3\hat{D}D_2 & -I \end{bmatrix} < 0 \tag{6}$$

$$\begin{bmatrix} Z & I \\ I & H \end{bmatrix} > 0 \tag{7}$$

Such that,

$$\begin{aligned} &\widehat{A} \triangleq NA_cM^T + NB_cCZ + HBC_cM^T + H(A + BD_cC)Z,\ \widehat{B} \triangleq NB_c + HBD_c, \\ &\widehat{C} \triangleq C_cM^T + D_cCZ,\ \widehat{D} \triangleq D_c,\ r \triangleq e^{(1-\hat{q})j\frac{\pi}{2}}. \end{aligned} \tag{8}$$

The term ϖ_i represents lumped uncertainties. Given that fuzzy weights and system states belong to compact sets, there exists a constant $\bar{\varpi}$ such that $\|\varpi_i\| \leq \bar{\varpi}$. The cross terms $\hat{C}\hat{D}^T$ and $\hat{D}\hat{C}^T$ represent symmetric coupling terms introduced during the LMI formulation. All matrices are assumed to be of compatible dimensions. The saturation nonlinearity is incorporated using the sector-bounded representation and multiplier matrix Γ, ensuring convexity of the resulting LMI conditions. The term $r(\cdot)$ denotes a bounded auxiliary vector function that captures residual approximation errors and uncertainty terms appearing in the closed-loop dynamics. It should be noted that the term $r = e^{(1-\hat{q})j\pi/2}$ arises from the frequency-domain representation of the fractional-order operator.

Theorem 1: *Considering the N-coupled FO system 1, when the control strategies and compensators are represented as:*

$$u_i = \frac{\left[-\sum_{j=1}^{N} a_{ij}\left(\hat{f}_j - \hat{f}_i\right) - \sum_{j=1, j\neq i}^{N} a_{ij}u_j - b_i D_t^{\hat{q}} x_0^n - K^T\hat{e}_i + u_{s,i}\right]}{-\sum_{j=1, j\neq i}^{N} a_{ij} - b_i}$$

$$D_t^{\hat{q}} x_{ci} = A_{ci}x_{ci} + B_{ci}e_i^t,\quad u_{s,i} = C_{ci}x_{ci} + D_{ci}e_i^t$$

Additionally, the maximum limit of the compensator is given by:

$$u_{s,i} \leq \frac{1}{|e_i^t| + c}\left|e_i^t\right|\|E_i\| \tag{9}$$

Then according to Lemma 1, the system is stable, in which u_i represents the control signal, and u_s denotes the compensator signal. The parameters a_{ij} and b_i define the communication topology, while $\hat{f}$ corresponds to the output. x_0 represent the leader's state. Additionally, $\hat{e}_i$ is error (see Eq. (11)). $|\hat{E}_i|$ denotes the maximum limit of the approximation error. The matrices A_{ci}, B_{ci}, C_{ci}, and D_{ci} are given as follows:

$$D_{ci} = \hat{D}, \quad C_{ci} = \left(-D_k CX + \hat{C}\right) M^{-T},$$
$$B_{ci} = N^{-1}\left(-HBD_{ci} + \hat{B}\right), \quad A_{ci} = N^{-1}\left(-HBC_{ci}M^T - NB_{ci}CX - H\left(A + BD_{ci}C\right)X + \hat{A}\right) M^{-T}.$$

Proof: For each node i, the local neighborhood tracking errors are defined as follows:

$$e_i = \sum_{j=1}^{N} a_{ij}(x_i - x_j) + b_i(x_i - x_0), \tag{10}$$

where a_{ij} are the elements of the adjacency matrix, b_i denotes the leader adjacency weight, and x_0 represents the leader's state. According to Eq. (10), the estimated tracking errors are formulated as follows:

$$\hat{e}_i^1 = \sum_{j\in N} a_{ij}\left(\hat{x}_j^1 - \hat{x}_i^1\right) + b_i\left(\hat{x}_0^1 - \hat{x}_i^1\right) \quad \cdots, \quad \hat{e}_i^n = \sum_{j\in N} a_{ij}\left(\hat{x}_j^n - \hat{x}_i^n\right) + b_i\left(x_0^n - x_i^n\right) \tag{11}$$

Here, $\hat{x}_i^1, \ldots, \hat{x}_i^n$ represent the estimations of $x_i^1, \ldots, x_i^n$, respectively, while $\hat{e}_i^1, \ldots, \hat{e}_i^n$ correspond to the estimations of $e_i^1, \ldots, e_i^n$, respectively. Apllying D_t^q and $D_t^{\hat{q}}$, Eqs. (10) and (11) results in:

$$D_t^q e_i^1 = \sum_{j\in\mathcal{N}} a_{ij}\left(D_t^q x_j^1 - D_t^q x_i^1\right) + b_i\left(D_t^q x_0^1 - D_t^q x_i^1\right), \ldots, D_t^q e_i^n = \sum_{j\in\mathcal{N}} a_{ij}\left(D_t^q x_j^n - D_t^q x_i^n\right) + b_i\left(D_t^q x_0^n - D_t^q x_i^n\right), \tag{12}$$

$$D_t^{\hat{q}} e_i^1 = \sum_{j\in\mathcal{N}} a_{ij}\left(D_t^{\hat{q}} \hat{x}_j^1 - D_t^{\hat{q}} \hat{x}_i^1\right) + b_i\left(D_t^{\hat{q}} x_0^1 - D_t^{\hat{q}} \hat{x}_i^1\right), \ldots, D_t^{\hat{q}} e_i^n = \sum_{j\in\mathcal{N}} a_{ij}\left(D_t^{\hat{q}} \hat{x}_j^n - D_t^{\hat{q}} \hat{x}_i^n\right) + b_i\left(D_t^{\hat{q}} x_0^n - D_t^{\hat{q}} \hat{x}_i^n\right), \tag{13}$$

where, $\hat{q}$ and $\hat{f}_i$ represent the estimated values of q and f_i. The saturation nonlinearity can be equivalently represented as $\text{sat}(u_i) = u_i + \Delta_i(u_i)$, where $\Delta_i(u_i)$ is a bounded dead-zone nonlinearity satisfying $\Delta_i(u_i)^T u_i \le 0, \quad \|\Delta_i(u_i)\| \le \bar{\Delta}_i$.

Put Eqs. (1) and (4) in Eqs. (12) and (13) and then by adding and subtracting $D_t^{\hat{q}}\hat{e}_i^1, \ldots, D_t^{\hat{q}}\hat{e}_i^n$ frome resulting Eq, one has:

$$\begin{aligned} &D_t^{\hat{q}}\tilde{e}_i^1 = \tilde{e}_i^2 + D_t^q e_i^1 - D_t^{\hat{q}} e_i^1, \quad D_t^{\hat{q}}\tilde{e}_i^2 = \tilde{e}_i^3 + D_t^q e_i^2 - D_t^{\hat{q}} e_i^2, \ldots, \\ &D_t^{\hat{q}}\tilde{e}_i^n = \textstyle\sum_{j=1}^{N} a_{ij}(f_j - \hat{f}_j + f_i - \hat{f}_i) + b_i(D_t^q x_0^n - D_t^{\hat{q}} x_0^n) + D_t^{\hat{q}} e_i^n - D_t^q e_i^n \end{aligned} \tag{14}$$

where,

$$\tilde{e}_i^1 = e_i^1 - \hat{e}_i^1, \tilde{e}_i^2 = e_i^2 - \hat{e}_i^2, \ldots, \tilde{e}_i^n = e_i^n - \hat{e}_i^n$$

Here, $f_i(\cdot)$ represents the unknown nonlinear dynamics of the i-th agent, while $\hat{f}_i(\cdot)$ denotes its approximation generated by the proposed RGT2FNN. Therefore, the term $f_i(\cdot) - \hat{f}_i(\cdot)$ represents the approximation error. We can reformulate these equations as follows:

$$D_t^{\hat{q}}\hat{e}_i = A\hat{e}_i + \zeta u_{si} + Lb_i, \tag{15}$$

$$D_t^{\hat{q}}\tilde{e}_i = \Omega\tilde{e}_i + E, \tag{16}$$

where, $\hat{e}_i = \left[\ \hat{e}_i^1, \ldots, \hat{e}_i^n\ \right]^T$, $\tilde{e}_i = \left[\ \tilde{e}_i^1, \ldots, \tilde{e}_i^n\ \right]^T$, $L = -\sum_{j=1}^{N} \Delta u_j$

$$A = \begin{bmatrix} 0 & 1 & 0 & \cdots & 0 \\ 0 & 0 & 1 & \cdots & 0 \\ \vdots & \vdots & \vdots & \ddots & \vdots \\ 0 & 0 & 0 & \cdots & 1 \\ -k_1 & -k_2 & -k_3 & \cdots & -k_n \end{bmatrix}, \quad \Omega = \begin{bmatrix} 0 & 1 & 0 & \cdots & 0 \\ 0 & 0 & 1 & \cdots & 0 \\ \vdots & \vdots & \vdots & \ddots & \vdots \\ 0 & 0 & 0 & \cdots & 1 \\ 0 & 0 & 0 & \cdots & 0 \end{bmatrix}, \quad \zeta = \begin{bmatrix} 0 \\ 0 \\ \vdots \\ 0 \\ 1 \end{bmatrix}$$

$$E_i = \begin{bmatrix} D_t^{\hat{q}} e_i^1 - D_t^q e_i^1, \\ D_t^{\hat{q}} e_i^2 - D_t^q e_i^2, \\ \vdots \\ \sum_{j=1}^{N} a_{ij} \left(f_j - \hat{f}_j + f_i - \hat{f}_i \right) + b_i \left(D_t^q x_0^n - D_t^{\hat{q}} x_0^n \right) + D_t^{\hat{q}} e_i^n - D_t^q e_i^n \end{bmatrix} \tag{17}$$

From Eqs. (15) and (16), one has:

$$D_t^{\hat{q}} \begin{bmatrix} \tilde{e}_i \\ \hat{e}_i \end{bmatrix} = \begin{bmatrix} \Omega & \underline{0} \\ \underline{0} & A \end{bmatrix} \begin{bmatrix} \tilde{e}_i \\ \hat{e}_i \end{bmatrix} + \begin{bmatrix} \underline{0} \\ \underline{1} \end{bmatrix} u_{si} + \begin{bmatrix} \underline{0} \\ L \end{bmatrix} b_i + \begin{bmatrix} B_i \\ \underline{0} \end{bmatrix} \varpi_i \tag{18}$$

where, $\underline{0}$ and $\underline{1}$ represent vectors consisting of zero and one elements, respectively. The terms B_i and ϖ_i are given by: $B_i \varpi_i = E_i$, $\quad \varpi_i \leq 1$. To guarantee robustness against the lumped uncertainty E (derived from ϖ_i) in Eq. (18), the compensator u_s is designed such that the LMI condition Eq. (6) ensures H_∞ performance, suppressing the influence of E on the error dynamics by a factor of γ. Eq. (18) is reformulated as follows:

$$D_t^{\hat{q}} \chi_i = A_1 \chi_i + B_1 u_{si} + B_2 \varpi_i + B_3 b_i, \quad y = C_1 \chi_i, \quad z = C_2 \chi_i$$

where,

$$\chi_i = \begin{bmatrix} \tilde{e}_i \\ \hat{e}_i \end{bmatrix}, \quad A_1 = \begin{bmatrix} \Omega & \underline{0} \\ \underline{0} & A \end{bmatrix}, \quad B_1 = \begin{bmatrix} \underline{0} \\ \underline{1} \end{bmatrix}, \quad B_2 = \begin{bmatrix} B_i \\ \underline{0} \end{bmatrix}, \quad B_3 = \begin{bmatrix} \underline{0} \\ L \end{bmatrix}, \quad C_1 = C_2 = \begin{bmatrix} \underline{0} & \underline{1} \end{bmatrix}$$

By resolving the LMI (6) and finding M and N that fulfill $MN^T = I - ZH$, the compensator matrices are derived from Eq. (8). The Lyapunov–Krasovskii functional is constructed as

$$V_i(t) = \frac{1}{2} \chi_i^T(t) \chi_i(t) + \frac{1}{2} \int_{t-\tau_i(t)}^{t} \chi_i^T(s) R \chi_i(s) ds,$$

where $R = R^T > 0$. Using the generalized fractional Leibniz rule and the boundedness condition $0 \leq \dot{\tau}_i(t) \leq \mu < 1$, the delay-dependent term can be estimated as

$$D_t^{\hat{q}} \int_{t-\tau_i(t)}^{t} \chi_i^T(s) R \chi_i(s) ds \leq \chi_i^T(t) R \chi_i(t) - (1-\mu) \chi_i^T(t-\tau_i(t)) R \chi_i(t-\tau_i(t)).$$

Since $0 \leq \dot{\tau}_i(t) \leq \mu < 1$, the delay term is negative semi-definite. Applying Young's inequality to the disturbance term yields

$$2 \chi_i^T B_2 \varpi_i \leq \chi_i^T B_2 B_2^T \chi_i + \varpi_i^T \varpi_i.$$

Because $\varpi_i^T \varpi_i \leq 1$, the derivative satisfies $D_t^{\hat{q}} V_i \leq \chi_i^T \Theta \chi_i$, where $\Theta = A_1^T + A_1 + R + B_2 B_2^T + B_1 K_s + K_s^T B_1^T$.

The system is asymptotically stable if there exist matrices $R = R^T > 0, \quad K_s, \quad \gamma > 0$ such that the following LMI holds:

$$\begin{bmatrix} A_1^T + A_1 + R & B_2 & B_1 \\ B_2^T & -I & 0 \\ B_1^T & 0 & -\gamma I \end{bmatrix} < 0.$$

Once the LMI is feasible, the LMI-based compensator is obtained as $u_{s,i} = -K_s \chi_i$, which guarantees $D_t^{\vartheta} V_i < 0$, ensuring consensus tracking and bounded closed-loop signals despite time-varying delays, actuator saturation, and RGT2FNN approximation errors. □

6 Simulation

This section assesses the efficiency of the proposed approach through example.

The proposed controller is implemented in a system consisting of five followers. The network topology is illustrated in Fig. 3. The leader's dynamics, along with the followers, are given as:

$$\begin{cases} D_t^{0.95} x_i^1 = x_i^2, \\ D_t^{0.95} x_i^2 = -0.1 x_i^1(t-\tau) + 0.4 x_i^2(t-\tau) + 5\sin(1.5t) + 8\cos(0.8t) + 2. \end{cases}$$

$$\begin{cases} D_t^{0.95} x_1^1 = x_1^2, \\ D_t^{0.95} x_1^2 = -0.1 x_1^1(t-\tau) + 0.4 x_1^2(t-\tau) + 5\sin(1.5t) + 8\cos(0.8t) \\ + 0.02\sin(0.5t) + 2 + u(t). \end{cases}$$

in which $\tau = 0.001$, ICs: $x_0(0) = [0, 0]$, $x_1(0) = [2, 0]$, $x_2(0) = [-2, 0]$, $x_3(0) = [3, 0]$, $x_4(0) = [-3, 0]$ and $x_5(0) = [4, 0]$, $K = [300, 30]^T$.

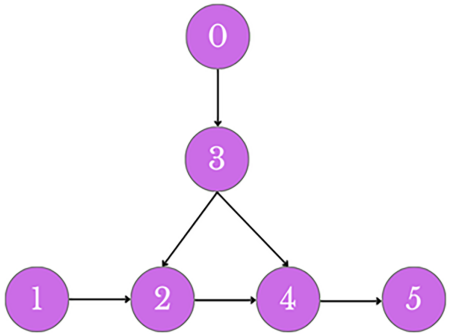

Figure 3: The tracking performance of all agents.

Fig. 4 shows the tracking performance, and it is noted that the trajectories of all the followers converge to the trajectory of the leader. Fig. 5 shows a three-dimensional representation of the paths of the agents in the coming together of their movement towards that of the leader. Type-2 fuzzy membership functions used in the RGT2FNN for uncertainty modeling are depicted in Fig. 6.

Fig. 7 presents the Lyapunov candidate function and its corresponding time derivative, providing a clear visualization of system stability under the designed control strategy. Following this, Fig. 8 demonstrates the control inputs applied to the system, highlighting how the proposed controller effectively enforces actuator saturation limits. The resulting tracking performance is further illustrated in Fig. 9, where the error trajectories of all agents are shown to converge to zero, confirming the efficacy of the proposed approach. Finally, Fig. 10 depicts the output surface generated by the GT2-FNN,

emphasizing its capability to accurately approximate complex nonlinear functions within the multi-agent system.

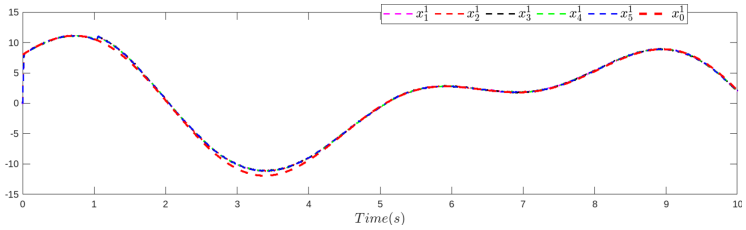

Figure 4: The tracking performance of all agents.

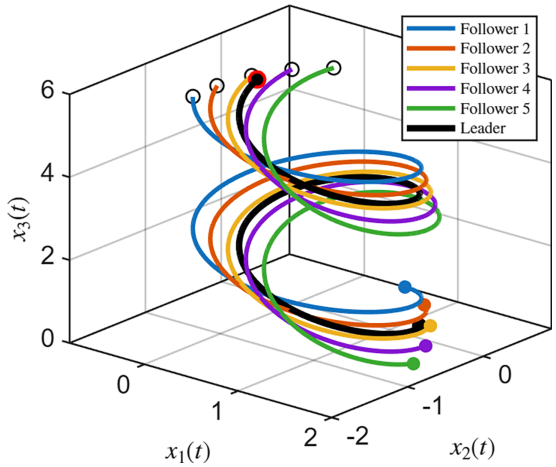

Figure 5: 3-D tracking performance of all agents.

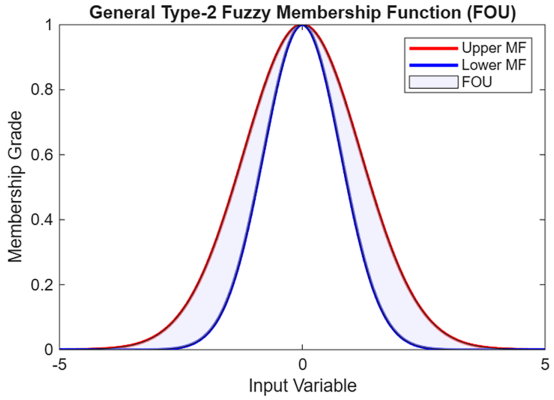

Figure 6: Fuzzy membership function.

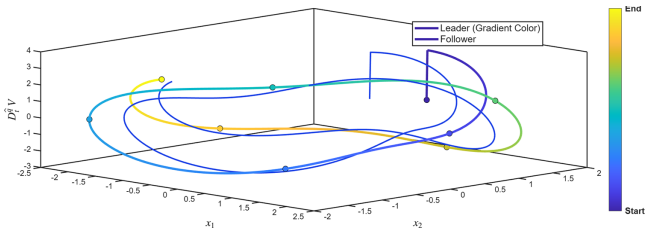

Figure 7: Lyapunov function and its time derivative.

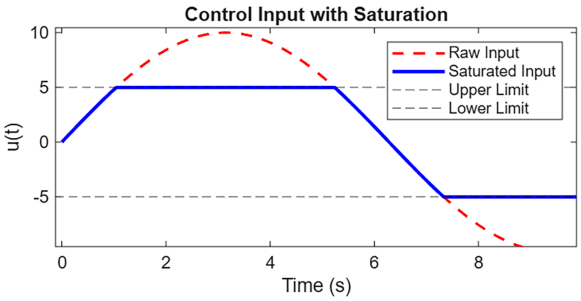

Figure 8: Control input with saturation.

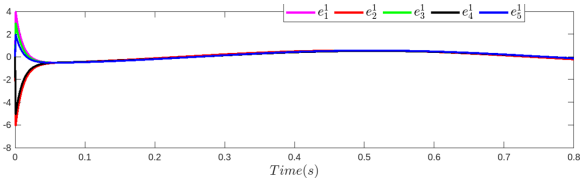

Figure 9: The tracking errors in all agents.

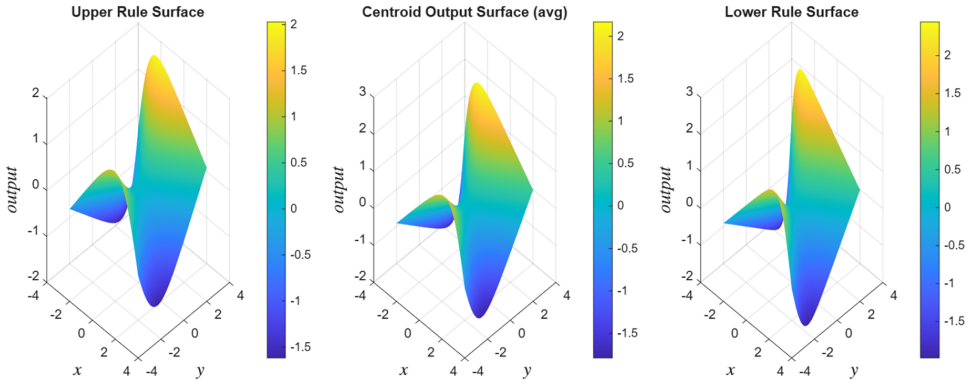

Figure 10: GT2-FNN output surface.

7 Conclusion

For fractional-order multi-agent systems with time-varying delays and input saturation constraints, a reliable adaptive control protocol was created in this work. The agents' unknown nonlinear

dynamics were precisely estimated by employing an RGT2FNN. A major gap in the existing literature was filled by the simultaneous identification of network parameters and fractional orders made possible by the application of the BBO optimization algorithm. The suggested framework guarantees consensus tracking and stability in spite of physical limitations and high model uncertainty, according to simulation results. The integrated approach of using BBO for order identification alongside an RGT2FNN for dynamic compensation presents a significant advancement over existing robust LMI-based controllers, particularly for applications requiring simultaneous handling of fractional orders, delays, and saturation.

Acknowledgement: This work has been carried out at the Hefei Technology College, China, University of Lahore, Sargodha Campus, Pakistan. The authors are also grateful for the support from King Faisal University Saudi Arabia.

Funding Statement: This article is supported by the Natural Science Research Project of the Department of Education of Anhui Province under Grant 2023AH052548, the National Natural Science Foundation of China under Grant 12301185. This work was supported by the Deanship of Scientific Research, Vice Presidency for Graduate Studies and Scientific Research, King Faisal University, Saudi Arabia [Grant No. KFU261358].

Author Contributions: Conceptualization, Ping Yu; Software, Salma Trabelsi; Validation, Salma Trabelsi; Formal analysis, Ping Yu; Resources, Ping Yu; Writing—original draft, Ping Yu and Hafiza Tabinda Rauf; Writing—review & editing, Hafiza Tabinda Rauf and Meraa Arab; Supervision, Meraa Arab and Ping Yu; Project administration, Ping Yu and Meraa Arab. All authors reviewed and approved the final version of the manuscript.

Availability of Data and Materials: The data that support the findings of this study are available from the corresponding author, Hafiza Tabinda Rauf, upon reasonable request.

Ethics Approval: Not applicable.

Conflicts of Interest: The authors declare no conflicts of interest.

References

1. Shi Y, Hou X, Na Z, Zhou J, Yu N, Liu S, et al. Bio-inspired attachment mechanism of dynastes hercules: vertical climbing for on-orbit assembly legged robots. J Bionic Eng. 2024;21(1):137–48. doi:10.1007/s42235-024-00485-8.
2. Du G, Zhang H, Yu H, Hou P, He J, Cao S, et al. Study on automatic tracking system of microwave deicing device for railway contact wire. IEEE Trans Instrum Meas. 2024;73:3527611. doi:10.1109/TIM.2024.3446638.
3. Hu J, Chen B, Ghosh BK. Formation-circumnavigation switching control of multiple ODIN systems via finite-time intermittent control strategies. IEEE Trans Control Netw Syst. 2024;11(4):1986–97. doi:10.1109/TCNS.2024.3371597.
4. Zhang C, Liu M, Liu Z, Sabetahd R, Taghavifar H, Mohammadzadeh A. A multiple model type-3 fuzzy control for offshore wind turbines using the Active Rotary Inertia Driver (ARID). Ocean Eng. 2024;313:119337. doi:10.1016/j.oceaneng.2024.119337.

5. Qi H, Ding L, Zheng M, Huang L, Gao H, Liu G, et al. Variable wheelbase control of wheeled mobile robots with worm-inspired creeping gait strategy. IEEE Trans Robot. 2024;40:3271–89. doi:10.1109/TRO.2024.3400947.
6. Ma Q, Xu S. Intentional delay can benefit consensus of second-order multi-agent systems. Automatica. 2023;147:110750. doi:10.1016/j.automatica.2022.110750.
7. Zeng Z, Zhu C, Goetz SM. Fault-tolerant multiparallel three-phase two-level converters with adaptive hardware reconfiguration. IEEE Trans Power Electron. 2024;39(4):3925–30. doi:10.1109/TPEL.2024.3350186.
8. Li S, Yang J, Bao H, Xia D, Zhang Q, Wang G. Cost-sensitive neighborhood granularity selection for hierarchical classification. IEEE Trans Knowl Data Eng. 2025;37(8):4471–84. doi:10.1109/TKDE.2025.3566038.
9. Zhou Z, Wang Y, Liu X, Li Z, Wu M, Zhou G. Hybrid of neural network and physics-based estimator for vehicle longitudinal dynamics modeling using limited driving data. IEEE Trans Intell Transp Syst. 2025;26(10):16735–46. doi:10.1109/TITS.2025.3585346.
10. Luan Z, Zhao W, Wang C. Coordinated tracking control of the integrated wheel-end system based on generalized instantaneous steering center constraint. IEEE Trans Transp Electrif. 2025;11(3):8271–81. doi:10.1109/TTE.2025.3538892.
11. Chen J, Li M, Marcantoni M, Jayawardhana B, Wang Y. Range-only distributed safety-critical formation control based on contracting bearing estimators and control barrier functions. IEEE Internet Things J. 2025;12(19):40968–79. doi:10.1109/JIOT.2025.3590774.
12. Wang B, Sun J, Peng B, Cui X, Cheng L, Zheng X. Optimal event-triggered neural learning tracking control for pneumatic muscle antagonistic joint with asymmetric constraints. IEEE Trans Ind Electron. 2025;72(12):14677–87. doi:10.1109/TIE.2025.3585055.
13. Liu J, Jiang G, Chu C, Li Y, Wang Z, Hu S. A formal model for multiagent Q-learning on graphs. Sci China Inf Sci. 2025;68(9):192206. doi:10.1007/s11432-024-4289-6.
14. Xiong JJ, Wang XY, Li C. Recurrent neural network based sliding mode control for an uncertain tilting quadrotor UAV. Int J Robust Nonlinear Control. 2025;35(18):8030–46. doi:10.1002/rnc.70108.
15. Li S, Wang S, Zhang Y, Wang X, Zhang Y, Wu W, et al. Distributed bearing-based fault-tolerant formation control of fixed-wing UAV swarm with prescribed performance. Aerosp Sci Technol. 2025;168(C):110897. doi:10.1016/j.ast.2025.110897.
16. Zhou L, Li Z, Li Y, Bai S. Parallel MPPI with gradient-velocity modulated SDF cost for high-performance real-time dynamic obstacle avoidance by robot manipulators. IEEE Trans Robot. 2025;41(6):5149–68. doi:10.1109/TRO.2025.3600125.
17. Mendel JM. General type-2 fuzzy logic systems made simple: a tutorial. IEEE Trans Fuzzy Syst. 2013;22(5):1162–82. doi:10.1109/TFUZZ.2013.2286414.
18. Aguila-Camacho N, Duarte-Mermoud MA, Gallegos JA. Lyapunov functions for fractional order systems. Commun Nonlinear Sci Numer Simul. 2014;19(9):2951–7. doi:10.1016/j.cnsns.2014.01.022.
19. Fadiga L, Farges C, Sabatier J, Santugini K. H_∞ output feedback control of commensurate fractional order systems. In: 2013 European Control Conference (ECC); 2013 Jul 17–19; Zurich, Switzerland. p. 4538–43. doi:10.23919/ECC.2013.6669646.
20. Kang Y, Yao L, Wang H. Fault isolation and fault-tolerant control for Takagi-Sugeno fuzzy time-varying delay stochastic distribution systems. IEEE Trans Fuzzy Syst. 2021;30(4):1185–95. doi:10.1109/TFUZZ.2021.3053320.
21. Hou M, Zhao J, Tian J, Du H. Minimum operator-based data-driven sliding mode control for a magnetorheological fluid dual clutch. IEEE Trans Cybern. 2025;55(10):4991–5001. doi:10.1109/TCYB.2025.3596063.
22. Liu R, Fan Y, Huang Y, Guo H, Zhao C, Su M. Design and workspace analysis of a cable-driven space capture robot for noncooperative targets. Proc Inst Mech Eng Part G J Aerosp Eng. 2024;238(14):1406–18. doi:10.1177/095441002412728.

23. Gao Y, Tahir M, Siano P, Hussain S, Sun W, He Y, et al. A bi-level hybrid game framework for Stochastic Robust optimization in multi-integrated energy microgrids. Sustain Energy Grids Netw. 2025;44:102024. doi:10.1016/j.segan.2025.102024.
24. Fu Y, Wang B, Zhao H, Zhou M, Li N, Gao Z. Adaptive safety attitude control of a hybrid VTOL UAV under transition flight subject to multiple faults and uncertainties. Aerosp Sci Technol. 2025;163:110284. doi:10.1016/j.ast.2025.110284.
25. Xu F, Feng S, Wang Y, Chang J, Zhou C. Efficient deep reinforcement learning with expert demonstrations for human-machine shared steering control under emergency obstacle avoidance conditions. IEEE Trans Veh Technol. 2025. doi:10.1109/TVT.2025.3629701.
26. Yang X, Puig V, Wang X, Wang S, Sun C, Zhang Y. Dynamic-high-gain-based decentralized optimal fault-tolerant control for a class of interconnected nonlinear systems. IEEE Trans Automat Contr. 2025;70(9):5823–35. doi:10.1109/TAC.2025.3546545.
27. Zhang Y, Wang Y, Su C, Miao Y, Wei T, Feng Y, et al. Multi-sensor fusion-based intelligent auxiliary system of power wheelchairs for individuals with limbs disabilities: design and implementation. Measurement. 2025;257(A):118573. doi:10.1016/j.measurement.2025.118573.
28. Song DN, Tang WC, Zhao YN, Zhong YG, Ma JW. Convolution-based velocity-smoothing principle and its application to real-time parametric curve interpolation. IEEE Trans Autom Sci Eng. 2025;22:23443–54. doi:10.1109/TASE.2025.3625244.
29. Gu J, Wang Y. A constrained reinforcement learning based approach for cooperative control of multi-UAV in dense obstacle environments. Sci China Technol Sci. 2026;69(1):1120601. doi:10.1007/s11431-025-3076-2.
30. Zhang J, Zhao X, Zheng G, Zhu F, Dinh TN. On distributed prescribed-time unknown input observers. IEEE Trans Automat Contr. 2025;70(7):4743–50. doi:10.1109/TAC.2025.3536856.
31. Zhang J, Song Y, Zheng G. Prescribed-time observer for descriptor systems with unknown input. Automatica. 2025;172(3):111999. doi:10.1016/j.automatica.2024.111999.
32. Zhang J, Zhao X, Zhu F, Karimi HR. Reduced-order observer design for switched descriptor systems with unknown inputs. IEEE Trans Automat Contr. 2019;65(1):287–94. doi:10.1109/TAC.2019.2913050.
33. Yan Z, Pan Z, Hu G, Yan H. Finite-time annular domain guaranteed cost control for uncertain mean-field stochastic systems with wiener and poisson noises. IEEE Trans Syst Man Cybern Syst. 2025;55(11):7981–93. doi:10.1109/TSMC.2025.3598993.
34. Zheng H, Lu J, Zhen S, Liu X, Chen YH. Hybrid nominal-robust control strategy with error-bounding constraints for enhanced hub motor performance. Control Eng Pract. 2026;168(3):106672. doi:10.1016/j.conengprac.2025.106672.
35. Ejegwa PA, Kausar N, Agba JA, Ugwuh F, Özbilge E, Ozbilge E. Determination of medical emergency via new intuitionistic fuzzy correlation measures based on Spearman's correlation coefficient. AIMS Math. 2024;9(6):15639–70. doi:10.3934/math.2024755.
36. Kausar N, Garg H. Contra-hormonic generalized fuzzy numerical scheme for solving mechanical engineering problems. J Appl Math Comput. 2024;70(5):4629–53. doi:10.1007/s12190-024-02148-7.
37. Yang Z, Kou J, Li Z, Ma Y, Zhao W, Wang Y, et al. Observer-based adaptive neural network force tracking control for pneumatic polishing system end-effector with actuator saturation. Neurocomputing. 2025;633(2):129824. doi:10.1016/j.neucom.2025.129824.